IOP Publishing Journal of Physics G: Nuclear and Particle Physics
J. Phys. G: Nucl. Part. Phys. **47** (2020) 035101 (15pp) https://doi.org/10.1088/1361-6471/ab5774

Constraints and correlations of nuclear matter parameters from a density-dependent van der Waals model

M Dutra[1,3], B M Santos[2] and O Lourenço[1]

[1] Departamento de Física, Instituto Tecnológico de Aeronáutica, DCTA, 12228-900, São José dos Campos, SP, Brazil
[2] Universidade Federal do Acre, 69920-900, Rio Branco, AC, Brazil

E-mail: marianad@ita.br

Received 23 August 2019, revised 6 November 2019
Accepted for publication 13 November 2019
Published 22 January 2020

Abstract

A recently proposed density-dependent van der Waals model, with only 4 free parameters adjusted to fix binding energy, saturation density, symmetry energy, and incompressibility, is analyzed under symmetric and asymmetric nuclear matter constraints. In a previous paper, it was shown that this model is fully consistent with the constraints related to the binary neutron star merger event named GW170817 and reported by the LIGO and Virgo collaboration. Here, we show that it also describes satisfactorily the low and high-density regions of symmetric nuclear matter, with all the main constraints satisfied. We also found a linear correlation between the incompressibility and the skewness parameter, both at the saturation density and show how it relates to the crossing point presented in the incompressibility as a function of the density. In the asymmetric matter regime, other linear correlations are found, namely, the one between the symmetry energy (J) and its slope (L_0), and other one establishing the symmetry energy curvature as a function of the combination given by $3J–L_0$.

Keywords: nuclear matter, correlations, van der Waals model

(Some figures may appear in colour only in the online journal)

1. Introduction

An often-used approach to treat many-nucleon systems is to fit directly some of the many-nucleon observables, allowing the construction of thermodynamic equations of state to study

[3] Author to whom any correspondence should be addressed.

the infinite nuclear matter. Among the main models constructed through this procedure, one can mention the widely known nonrelativistic Skyrme model [1, 2]. For the relativistic case, on the other hand, a Lagrangian density is proposed and all thermodynamic quantities are derived from it. In its simplest version, the Walecka model [3–5], based on relativistic field theory in a mean-field approach, depends on free parameters fitted to reproduce the infinite nuclear matter bulk properties. The applications of these models extend to different ranges of temperature and density. For the zero temperature regime, the detailed knowledge of the hadronic equations of the state, coming from both, relativistic and nonrelativistic models, is very important for the description of, for example, neutron stars, which are studied in densities up to around six times the nuclear saturation density (ρ_0) [6, 7].

In the finite temperature regime, in which the hadronic models are generalized to $T \neq 0$ but keeping the adjustment of the free parameters performed at $T = 0$, the phenomenon of phase transitions in nuclear matter takes place. In general, hadronic models exhibit a liquid–gas phase transition characterized by regions presenting low (gas phase) and high (liquid phase) densities at a temperature range of $T \lesssim 20$ MeV [8, 9]. This is the typical feature presented by the known van der Waals (vdW) model [10, 11] in a temperature range of $T < T_c$, where T_c is the critical temperature. Such similarities pose the question of whether the vdW model could also be used to describe hadronic systems. In [12], the vdW model had its canonical ensemble thermodynamics converted into the grand canonical one. Later on, in [13], the authors performed a direct application of this model to the nuclear matter environment at zero and finite temperature regime. In [14], the authors used the same procedure adapting it to other real gases models (Redlich–Kwong–Soave, Peng–Robinson, and Clausius) to describe the infinite nuclear matter. However, these models present a limitation at high-density regime since they produce equations of state in which causality is violated for densities around $2.5\rho_0$ at most. Therefore, an important nuclear matter constraint, namely, the flow constraint [15], can not be reached since it is defined in the region of $2 \leqslant \rho/\rho_0 \leqslant 5$. Furthermore, the stellar matter can also not be described due to this limitation. The origin of such a problem is the absence of a suitable relativistic treatment of the hard-core repulsion, namely, the implementation of the Lorentz contraction (see, for instance [16]).

In [17], the authors considered a density-dependent vdW model in which the attractive and repulsive strengths were converted from constants to density-dependent functions properly chosen in order to avoid superluminal equations of state at low densities. It was shown that such a model, named as the DD-vdW model, is able to reproduce the flow constraint and also observational data of neutron stars. In particular, it was also shown that the constraints coming from the analysis of the GW170817 event, performed by the LIGO and Virgo collaboration, are fully satisfied by this model [18, 19]. In the present work, we focus on the analysis of the DD-vdW model against the symmetric and asymmetric nuclear matter constraints used in [20] to test 263 parametrizations of different relativistic mean-field (RMF) models. We also investigate the correlations between the bulk parameters presented by this model concerning the isoscalar and isovector sectors.

In section 2, we present the density-dependent perspective of the real gases models with the DD-vdW model properly described in section 3. The model is submitted to the constraints in section 4, and the summary and conclusions of this work are shown in section 5.

2. Real gases in a density dependent model perspective (nuclear matter description)

The classical vdW model in the canonical ensemble is expressed by the following equation of state for the pressure [10, 11],

$$P(\rho, T) = \frac{T\rho}{1 - b\rho} - a\rho^2, \tag{1}$$

in which the parameters a and b represent, respectively, the strength of the attractive and repulsive parts of the interaction between the hard-sphere particles of radius r. The excluded volume parameter b relates to r through $b = 16\pi r^3/3$, in the so-called exclude volume mechanism. The Redlich–Kwong–Soave [21, 22], the Peng–Robinson [23] and the Clausius models present the same expression for the first term on the right hand side of equation (1), but different structures for the second one.

In [13, 14], a suitable conversion of equation (1) to the grand canonical ensemble, with relativistic treatment, was performed in order to use the vdW model and the other real gases ones in the description of infinite nuclear matter. By taking such a procedure into account, it is possible to construct a unique formulation to all the real gases if one considers a suitable description in terms of density-dependent functions for the attractive and repulsive parts of the nuclear interaction. In this case, the energy density for the infinite symmetric nuclear matter (SNM) in the grand canonical ensemble reads [17]

$$\mathcal{E}(\rho) = [1 - b(\rho)\rho]\mathcal{E}^*_{\rm id}(\rho^*) - a(\rho)\rho^2, \tag{2}$$

with

$$\rho^* = \frac{\rho}{1 - b(\rho)\rho}. \tag{3}$$

The quantity $\mathcal{E}^*_{\rm id}$ is the kinetic energy of a relativistic ideal Fermi gas of nucleons of mass $M = 938$ MeV, given by

$$\mathcal{E}^*_{\rm id}(\rho^*) = \frac{\gamma}{2\pi^2}\int_0^{k_F^*} {\rm d}k\, k^2(k^2 + M^2)^{1/2}, \tag{4}$$

with $k_F^* = (6\pi^2\rho^*/\gamma)^{\frac{1}{3}}$. The degeneracy factor is $\gamma = 4$ for SNM.

The attractive interaction, now depending on ρ, assumes different forms for the real gases, namely,

$$a(\rho) = a \text{ (vdW)}, \tag{5}$$

$$a(\rho) = \frac{a}{b\rho}\ln(1 + b\rho) \text{ (RKS)}, \tag{6}$$

$$a(\rho) = \frac{a}{2\sqrt{2}\,b\rho}\ln\left[\frac{1 + b\rho(1 + \sqrt{2})}{1 + b\rho(1 - \sqrt{2})}\right] \text{(PR)}, \tag{7}$$

$$a(\rho) = \frac{a}{1 + b\rho} \text{ (C2)}, \tag{8}$$

for van der Waals (vdW), Redlich–Kwong–Soave (RKS), Peng–Robinson (PR), and Clausius-2 (C2) models. The last model is denoted by Clausius-2 since it is a two parameters version of the original Clausius model in which three parameters are considered [24]. For the repulsive interaction, on the other hand, it is possible to construct at least two possible forms

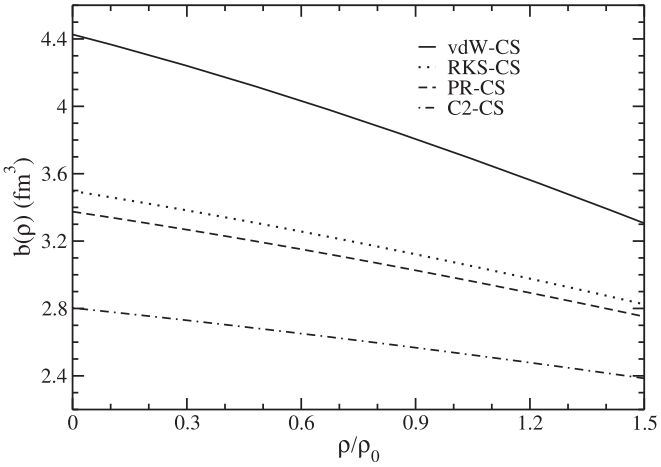

Figure 1. Density dependence of the repulsive interaction for the real gases submitted to the CS method of excluded volume, equation (11).

for all the real gases models. The first is related to the conventional excluded volume mechanism in which

$$b(\rho) = b, \tag{9}$$

i.e. a pure constant. Another form takes into account the Carnahan–Starling (CS) [25] method of excluded volume, in which the pressure of hard-core nucleons of radius r is given as $P = \rho T Z_{\rm CS}(\eta)$, with

$$Z_{\rm CS}(\eta) = \frac{1 + \eta + \eta^2 - \eta^3}{(1 - \eta)^3} = 1 + \sum_{j=0}^{\infty} (j^2 + 3j)\eta^j, \tag{10}$$

and $\eta = b\rho/4$. Using this method, we can find the first eight coefficients of the virial expansion unlike the traditional excluded volume method (EV), in which only two of them are recovered since, for this case, one has $Z(\eta) = (1–4\eta)^{-1}$. Such a procedure, used for the description of nuclear matter by the real gases models in [14], leads to the following density-dependent form for the repulsive interaction [17],

$$b(\rho) = \frac{1}{\rho} - \frac{1}{\rho}\exp\left[\frac{-\left(4 - \frac{3b\rho}{4}\right)\frac{3b\rho}{4}}{\left(1 - \frac{3b\rho}{4}\right)^2}\right]. \tag{11}$$

As one can see in figure 1, $b(\rho)$ is a decreasing function for all the real gases models submitted to the CS procedure.

For all the real gases models constructed with the EV or CS methods, there are only two free parameters to be adjusted, namely, the constants a and b, found in this case by imposing the binding energy value of $B_0 \approx 16.0$ MeV at the saturation density given by $\rho_0 \approx 0.16$ fm^{-3}. For the vdW-EV model, for instance, one has $a = 328.93$ MeV fm^3 and $b = 3.41$ fm^3 whereas for the vdW-CS model, these numbers change to 347.02 MeV fm^3 and 4.43 fm^3, respectively.

From equation (2), and by using the general relationship

$$\frac{\partial}{\partial\rho} = \frac{1 + b'\rho^2}{[1 - b(\rho)\rho]^2}\frac{\partial}{\partial\rho^*}, \tag{12}$$

coming from equation (3), the pressure of the system is obtained, namely,

$$\begin{aligned} P(\rho) &= \rho^2\frac{\partial(\mathcal{E}/\rho)}{\partial\rho} = \rho^2\frac{\partial}{\partial\rho}[\mathcal{E}^*_{\rm id}/\rho^* - a(\rho)\rho] \\ &= [1 - b(\rho)\rho]^2\rho^{*2}\frac{\partial(\mathcal{E}^*_{\rm id}/\rho^*)}{\partial\rho^*} - a'\rho^3 - a(\rho)\rho^2 \\ &= (1 + b'\rho^2)P^*_{\rm id} - a'\rho^3 - a(\rho)\rho^2 = P^*_{\rm id} - a(\rho)\rho^2 + \rho\Sigma(\rho), \end{aligned} \tag{13}$$

with

$$P^*_{\rm id} = \frac{\gamma}{6\pi^2}\int_0^{k_F^*}\frac{{\rm d}k\ k^4}{(k^2 + M^2)^{1/2}}. \tag{14}$$

Here, a' and b' are the density derivatives of $a(\rho)$ and $b(\rho)$, respectively, and the rearrangement term is

$$\Sigma(\rho) = b'\rho P^*_{\rm id} - a'\rho^2. \tag{15}$$

A generalization of the equation of state given in equation (2) to asymmetric nuclear matter, i.e. a system in which $y \equiv \rho_p/\rho \neq 1/2$ (ρ_p is the proton density), was proposed in [17]. It consists of adding a term proportional to the squared difference between protons and neutrons densities, namely, $\rho_3 = \rho_p - \rho_n$, as used widely in some RMF models [20]. The individual components (nucleons) are also distinguished by their respective kinetic energies. The final form for the energy density in this perspective is given by

$$\begin{aligned} \mathcal{E}(\rho, y) &= [1 - b(\rho)\rho]\mathcal{E}^*_{\rm id}(\rho^*_p, \rho^*_n) - a(\rho)\rho^2 \ + \ d\rho_3^2 \\ &= [1 - b(\rho)\rho]\mathcal{E}^*_{\rm id}(\rho^*_p, \rho^*_n) - a(\rho)\rho^2 \ + \ d(2y - 1)^2\rho^2, \end{aligned} \tag{16}$$

where $\mathcal{E}^*_{\rm id}(\rho^*_p, \rho^*_n) = \mathcal{E}^{*p}_{\rm id}(\rho^*_p) + \mathcal{E}^{*n}_{\rm id}(\rho^*_n)$, for $\mathcal{E}^{*i}_{\rm id}(\rho^*_i)$ following the same form as in equation (4) with $\gamma = 2, k^*_F \to k^{*i}_F$ and $\rho^* \to \rho^*_i$ ($i = p, n$). The different densities are related to each other by

$$\rho^*_p = \frac{\rho_p}{1 - b(\rho)\rho}, \qquad \rho^*_n = \frac{\rho_n}{1 - b(\rho)\rho}, \tag{17}$$

with $b(\rho)$ given in equation (11). An interpretation for this new term in equation (16) is that it mimics the ρ meson exchange between the finite structure nucleons.

3. DD-vdW model

An important limitation of the real gases models presented in the previous section is the production of superluminal equations of state at densities not so high in comparison with the saturation density. The maximum densities attained by these models immediately before the violation of the causal limit ($v_s^2 = \partial P/\partial\mathcal{E} > 1$) is presented in table 1 for the EV and CS method of excluded volume.

It is worth to note that the repulsive interaction plays an important role in the causal limit of the models since its density-dependent version induces the violation of causality at higher densities. The physical reason of this finding is that the CS method weakens the repulsive

Table 1. Maximum density ratio, $\rho_{\rm max}/\rho_0$, for the real gases models submitted to the two mechanisms of excluded volume, namely, EV and CS methods.

Model	$\rho^{\rm EV}_{\rm max}/\rho_0$	$\rho^{\rm CS}_{\rm max}/\rho_0$
vdW	1.38	1.69
RKS	1.58	2.07
PR	1.65	2.16
C2	1.84	2.51

Table 2. Maximum density ratio, $\rho_{\rm max}/\rho_0$, for some values of the n power, equation (18), of the DD-vdW model.

n	$\rho_{\rm max}/\rho_0$
0	1.69
1	2.51
2	3.74
3	5.16
4	6.61

interaction as a function of density, according to the results displayed in figure 1, producing results closer to those of an ideal gas of massive point-like nucleons. For this case, causality is not violated [17]. Even with this effect, the CS method is still not able to generate equations of state for densities greater than around $2.5\rho_0$, which is the best case of the C2-CS model. This result does not allow an analysis of the nuclear matter at high-density regime. Motivated by this limitation, it was proposed in [17] a new form for the attractive interaction, given by

$$a(\rho) = \frac{a}{(1 + b\rho)^n}. \tag{18}$$

It is inspired in the C2 model, where causality is violated at higher densities in comparison with the remaining models. The set of equations of state given in equations (2) and (13) for SNM, and (16) for the asymmetric case, with the repulsive and attractive interactions given by equations (11) and (18), respectively, was named as the DD-vdW model. Notice that for the particular cases of $n = 0$, and $n = 1$, the vdW-CS and C2-CS models are reproduced, respectively, see equations (5) and (8). In table 2, we show the limit density reached by this model for some values of the power n.

The effect of the n power in $a(\rho)$ is that it weakens the strength of the attractive interaction. Therefore, the model approaches the free Fermi gas of massive particles in which the condition $v_s^2 < 1$ is verified. The combined effect of the density-dependent parameters $a(\rho)$ and $b(\rho)$ enables the model to reach higher densities.

The additional free parameter of the DD-vdW model, n, is adjusted in order to correctly fix the value of the incompressibility at the saturation density, namely, $K_0 = 9(\partial P/\partial\rho)|_{\rho_0}$. For the real gases models in the CS method, this value is in the range of $333\,{\rm MeV} \leqslant K_0 \leqslant 601\,{\rm MeV}$ [14]. In [26, 27], a formulation including induced surface tension was implemented in the van der Waals model. The resulting approach also satisfies the flow constraint and the maximum mass observational data for neutron stars.

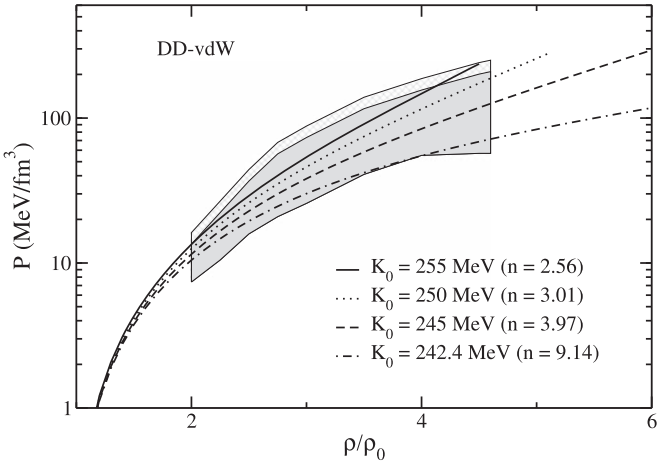

Figure 2. Pressure as a function of ρ/ρ_0 for different DD-vdW parametrizations. Bands: flow constraint described in [15, 20].

4. Constraints and correlations from the DD-vdW model

In this section, we proceed to analyze the DD-vdW model against the constraints used to select the 35 parametrizations of different RMF models out of 263 investigated in [20]. These selected parametrizations had their bulk and thermodynamical quantities compared to respective theoretical/experimental data from symmetric matter, pure neutron matter (PNM), and a mixture of both, namely, symmetry energy and its slope evaluated at the saturation density (J and L_0), and the ratio of the symmetry energy at $\rho_0/2$ to its value at ρ_0. We also investigate whether correlations between the bulk parameters also arise in the isoscalar and isovector sectors of the DD-vdW model.

4.1. Constraints in symmetric matter

As a first constraint, we analyze the region in the density dependence of the pressure determined in [15] from the analysis of the flow in the collisions of ^{197}Au. The result is depicted in figure 2.

In [17], the authors considered the region obtained in [15]. Here, we also take into account the 20% of increasing in this band as used in [20]. Such an increase was based on the band region obtained in [28] in which the authors performed an analysis based on observational data of bursting neutron stars showing photospheric radius expansion and transiently accreting neutron stars in quiescence. From the figure, one can verify that the parametrizations presenting $242.4\,\text{MeV} \leqslant K_0 \leqslant 255\,\text{MeV}$ are in full agreement with the flow constraint. Furthermore, such a range for K_0 also agrees with the constraint used in [20], namely, $190\,\text{MeV} \leqslant K_0 \leqslant 270\,\text{MeV}$. It also overlaps with the restriction for this quantity given by $250\,\text{MeV} \leqslant K_0 \leqslant 315\,\text{MeV}$ found in [29]. Furthermore, it is also consistent with the range recently discussed in [30], namely, $K_0 = (240 \pm 20)\,\text{MeV}$.

Another SNM constraint, coming from experiments of kaon production in heavy-ion collisions [31, 32], also defines a band in the density dependence of the pressure but now at $1.2 \leqslant \rho/\rho_0 \leqslant 2.2$. In figure 3, we show the behavior of the DD-vdW model against this constraint.

One can see that the DD-vdW model is also consistent with this particular constraint.

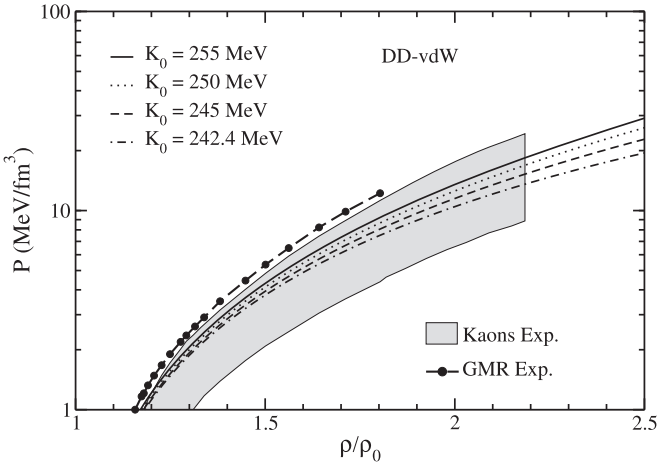

Figure 3. Pressure as a function of ρ/ρ_0 for the DD-vdW parametrizations consistent with the flow constraint. Band and circle-dashed line: experimental data extracted from the [31, 32].

4.2. Correlations in isoscalar sector

We also investigate for the DD-vdW model, a possible correlation between bulk parameters in the SNM, namely, the one involving K_0 and the skewness coefficient at the saturation density, $Q_0 = Q(\rho_0)$ with

$$Q(\rho) = 27\rho^3 \frac{\partial^3(\mathcal{E}/\rho)}{\partial\rho^3}. \tag{19}$$

The skewness coefficient is a bulk parameter that directly affects the high-density behavior of a hadronic model. In [33], for instance, the authors provide a detailed studied showing the impact of Q_0 in the RMF hadronic model. Different parametrizations with the same bulk parameters excepting the skewness coefficient were used to investigate the specific role played by Q_0 in the flow constraint and mass-radius diagram of neutron stars [33].

In order to examine a possible relationship between Q_0 and K_0, we proceed here as in [34] where the authors have shown that a signature of linear correlations is exhibited in the density dependence of the bulk parameter analyzed. For instance, if we look for the density dependence of $K(\rho)$, and if a crossing point arises, consequently it generates to the linear relation between Q_0 and K_0. Actually, in figure 4 we show that this is the case for the DD-vdW model.

From the expansion of the energy per particle given by,

$$\frac{\mathcal{E}}{\rho} \simeq -B_0 + \frac{K_0}{2!}x^2 + \frac{Q_0}{3!}x^3 + \cdots, \tag{20}$$

with $x = \frac{\rho-\rho_0}{3\rho_0}$, we found

$$\begin{aligned} K(\rho) &= 18\rho\frac{\partial(\mathcal{E}/\rho)}{\partial\rho} + 9\rho^2\frac{\partial^2(\mathcal{E}/\rho)}{\partial\rho^2} = 6(3x+1)\frac{\partial(\mathcal{E}/\rho)}{\partial x} + (3x+1)^2\frac{\partial^2(\mathcal{E}/\rho)}{\partial x^2} \\ &\simeq (3x+1)[K_0 + (9K_0 + Q_0)x + 6Q_0x^2]. \end{aligned} \tag{21}$$

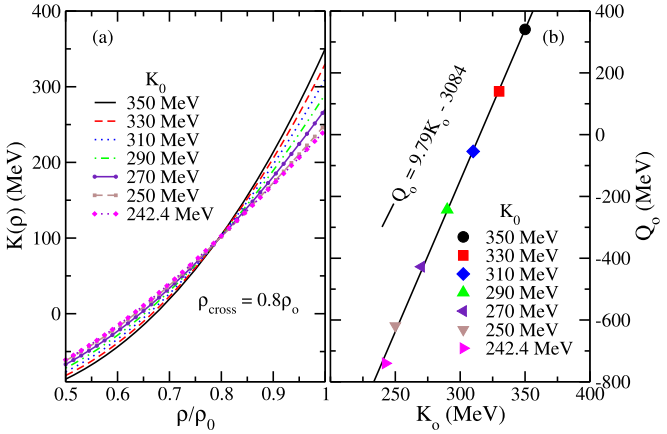

Figure 4. (a) Incompressibility as a function of ρ/ρ_0 for some DD-vdW parametrizations. The density in which the parametrizations cross each other is given by $\rho_{\rm cross}$. (b) $Q_0 \times K_0$ linear correlation observed for the same parametrizations. Solid line: fitting curve.

If the following linear correlation is true,

$$Q_0 = a_1 K_0 + a_2, \tag{22}$$

then

$$K(\rho) \simeq (3x + 1)[K_0 F(x) + (1 + 6x)a_2 x], \tag{23}$$

with $F(x) = 1 + (9 + a_1)x + 6a_1 x^2$, and $K(\rho_{\rm cross})$ will present the same value for different parametrizations only if one has $F(x_{\rm cross}) = 0$ for a particular point (crossing point) given by $\rho_{\rm cross} = (3x_{\rm cross} + 1)\rho_0$. Since we found this crossing point in figure 4(a), the correlation in equation (22) holds and the condition $F(x_{\rm cross}) = 0$ is satisfied, in this case for $\rho_{\rm cross}/\rho_0 = 0.8$ (also from figure 4(a)). The relationship between Q_0 and K_0 is exhibited in figure 4(b), confirming the linear correlation. A linear fitting points out to $a_1 = 9.79$, generating the more accurate value of $\rho_{\rm cross}/\rho_0 = 0.798$, coming from the exact solution of $F(x_{\rm cross}) = 0$. The authors of [35] also found a crossing for some nonrelativistic Skyrme and Gogny parametrizations, with $\rho_{\rm cross}/\rho_0 = 0.7$. However, for the RMF models analyzed, they did not find any linear correlations or even crossing points. In this case, this is due to the different values of the effective nucleon mass for the distinct parametrizations, as explained in [34]. However, for Boguta–Bodmer models in which effective mass is $0.6M$, for instance, one has a crossing in the $K(\rho)$ curve at $\rho_{\rm cross}/\rho_0 = 0.77$ and, as a consequence, a linear correlation between Q_0 and K_0 [34]. The crossing density found in the DD-vdW model is close to the values obtained by the aforementioned models.

For the DD-vdW parametrizations in which the flow constraint is satisfied, the respective Q_0 values are in the range of -740 MeV $\leqslant Q_0 \leqslant -569$ MeV, which is compatible with other calculations giving -690 MeV $\leqslant Q_0 \leqslant -208$ MeV [36], -790 MeV $\leqslant Q_0 \leqslant -330$ MeV [36], and -1200 MeV $\leqslant Q_0 \leqslant -200$ MeV [37].

4.3. Asymmetric matter

In the SNM, the DD-vdW model contains only three free parameters, namely, the constants a, b and n present in equations (11) and (18). In the generalization to asymmetric matter proposed in equation (16), there is one more free constant, namely, the d parameter. In [17],

this constant was adjusted in order to fix the symmetry energy at the saturation density, $J \equiv \mathcal{S}(\rho_0)$, where

$$\mathcal{S}(\rho) = \frac{1}{8}\frac{\partial^2(\mathcal{E}/\rho)}{\partial y^2}\bigg|_{y=\frac{1}{2}} = \mathcal{S}^*_{\rm kin}(\rho) + d\rho, \tag{24}$$

with $\mathcal{S}^*_{\rm kin}(\rho) = k_{\rm F}^{*2}/(6E_{\rm F}^*)$ and $E_{\rm F}^* = \sqrt{k_{\rm F}^{*2} + M^2}$. The choice of fixing J in the range of 25 MeV $\leqslant J \leqslant$ 35 MeV automatically becomes the model consistent with the constraint used in [20], obtained from the data collection reported in [38].

From equation (24), one obtains the symmetry energy slope as follows,

$$L(\rho) = 3\rho\frac{\partial \mathcal{S}}{\partial \rho} = \xi(\rho)L^*_{\rm kin}(\rho) + 3d\rho, \tag{25}$$

where

$$L^*_{\rm kin}(\rho) = \frac{k_{\rm F}^{*2}}{3E_{\rm F}^*}\left(1 - \frac{k_{\rm F}^{*2}}{2E_{\rm F}^{*2}}\right) = 2\mathcal{S}^*_{\rm kin}\left(1 - \frac{3\mathcal{S}^*_{\rm kin}}{E_{\rm F}^*}\right), \tag{26}$$

and $\xi(\rho) = (1 + b'\rho^2)/[1 - b(\rho)\rho]$.

One advantage of the specific form of the last term added in the energy density in equation (16), namely, that one containing the d parameter, is that it generates an analytical relationship between $\mathcal{S}(\rho)$ and $L(\rho)$ for all densities, since one can write $d = (\mathcal{S} - \mathcal{S}^*_{\rm kin})/\rho$ from equation (24). This result leads to $L(\rho) = 3\mathcal{S}(\rho) + g(\rho)$, with

$$g(\rho) = \mathcal{S}^*_{\rm kin}(\rho)\left\{2\xi(\rho)\left[1 - \frac{3\mathcal{S}^*_{\rm kin}(\rho)}{E_{\rm F}^*(\rho)}\right] - 3\right\} \tag{27}$$

i.e. a linear correlation between $L(\rho)$ and $\mathcal{S}(\rho)$ is clearly established if $g(\rho)$ does not vary significantly.

A possible linear correlation at saturation density given by

$$L(\rho_0) \equiv L_0 \;\; = \;\; 3J + g_0 \tag{28}$$

is of great interest, since it is observed in many hadronic models [34, 39–41]. It will be satisfied if $g(\rho_0) \equiv g_0$ is approximately fixed regarding a variation of J. Indeed, this is the case for the DD-vdW parametrizations in which ρ_0, B_0 and K_0 are kept fixed for different values of J. The reason is that g_0 is a function of quantities depending only on free parameters adjusted from observables related to the symmetric matter, which means that g_0 depends only on ρ_0, B_0 and K_0, i.e. $g_0 = g_0(\rho_0, B_0, K_0)$. For parametrizations presenting these symmetric matter quantities fixed, independently of their J values, g_0 is a constant. This situation could not be the same if we had proposed terms in equation (16) with more than one isovector free parameter to be adjusted. The linear correlation in equation (28) can be blurred in this case since g_0 can also depend on J. However, some relativistic and nonrelativistic models with more than one isovector free parameter also present the same relationship of equation (28), as the NL3* [42] family and some Skyrme parametrizations, for instance [34, 43].

For DD-vdW parametrizations consistent with the flow constraint, namely, those in which 242.4 MeV $\leqslant K_0 \leqslant$ 255 MeV, we found the slope of symmetry energy at saturation density in the range of 63.4 MeV $\leqslant L_0 \leqslant$ 97.1 MeV, see figure 5(a). It was obtained from equation (28) and by taking into account the J constraint of 25 MeV $\leqslant J \leqslant$ 35 MeV. These L_0 values are in full agreement with constraint of 25 MeV $\leqslant L_0 \leqslant$ 115 MeV applied in the RMF parametrizations studied in [20], and obtained from the data collection presented in [38].

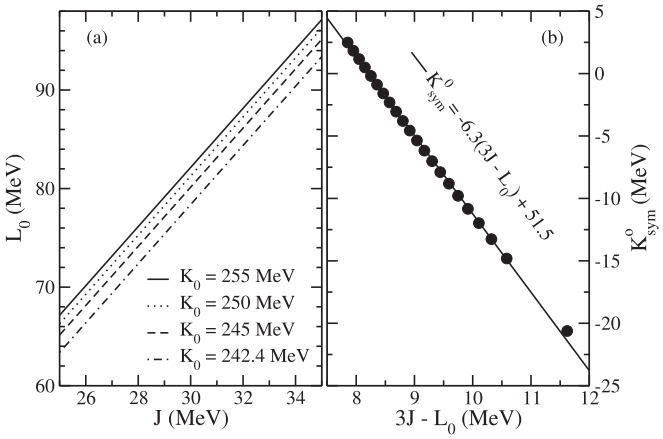

Figure 5. (a) L_0 as a function of J, and (b) $K^0_{\rm sym}$ as a function of $3J - L_0 = -g_0(\rho_0, B_0, K_0)$. The full circles were obtained by using the range of 242.4 MeV $\leqslant K_0 \leqslant$ 255 MeV, with fixed values of $\rho_0 = 0.16$ fm^{-3} and $B_0 = 16$ MeV. Both panels constructed from the DD-vdW parametrizations consistent with the flow constraint.

It is also possible to find analytic expressions for higher-order terms of $\mathcal{S}$ from equation (24). In particular, its curvature is given by

$$K_{\rm sym}(\rho) = 9\rho^2\frac{\partial^2\mathcal{S}}{\partial\rho^2} = 3\rho g'(\rho). \tag{29}$$

At the saturation density, we have $K^0_{\rm sym} = 3\rho_0 g'_0$, with $K^0_{\rm sym} \equiv K_{\rm sym}(\rho_0)$. Likewise g_0, the quantity g'_0 is a function only of the isoscalar bulk parameters of the model, i.e. $g'_0 = g'_0(\rho_0, B_0, K_0)$.

Notice that if the quantity g'_0 can be given also as a function of g_0 in a linear form as $g'_0 = \alpha_1 g_0 + \alpha_2$, then $K^0_{\rm sym}$ would be given by $K^0_{\rm sym} = 3\rho_0[-\alpha_1(3J - L_0) + \alpha_2]$, according to equation (28), i.e. a linear correlation between $K^0_{\rm sym}$ and $3J - L_0$ would arise (α_1 and α_2 are constants). Indeed, it is verified that g'_0 linearly depends on g_0 as one can see in figure 6. The black circles were obtained by using the values of $\rho_0 = 0.16$ fm^{-3}, $B_0 = 16$ MeV and running K_0 in the range of 242.4 MeV $\leqslant K_0 \leqslant$ 255 MeV. The direct consequence of the relationship between g'_0 and g_0 is the correlation between $K^0_{\rm sym}$ and $3J$–L_0 presented in figure 5(b), with a fitting curve given by $K^0_{\rm sym} = -6.3(3J - L_0) + 51.5$. As in figure 6, the full circles in figure 5(b) were calculated by using the range of 242.4 MeV $\leqslant K_0 \leqslant$ 255 MeV, with the aforementioned fixed values for ρ_0 and B_0. This linear correlation between $K^0_{\rm sym}$ and $3J - L_0$ was shown for 500 relativistic and nonrelativistic parametrizations in [44], and specifically for the Skyrme model in [45]. Also in [46], the authors have discussed such relationships. From this strong linear behavior, it is possible to obtain a range for the symmetry energy curvature for the DD-vdW parametrizations consistent with flow constraint, namely, -20.6 MeV $\leqslant K^0_{\rm sym} \leqslant 2.5$ MeV. This range is inside the one obtained for some RMF parametrizations in [44], according to figure 1 of this reference.

Another constraint adopted in [20, 47] was the one concerning the density dependence of PNM energy per particle (equation (16) evaluated at $y = 0$) at very low density regime. It was based on the lattice chiral effective theory including corrections due to finite scattering length, nonzero effective range, and higher-order corrections related to the nucleon–nucleon interaction in that regime. We submitted the DD-vdW model also to this constraint with results

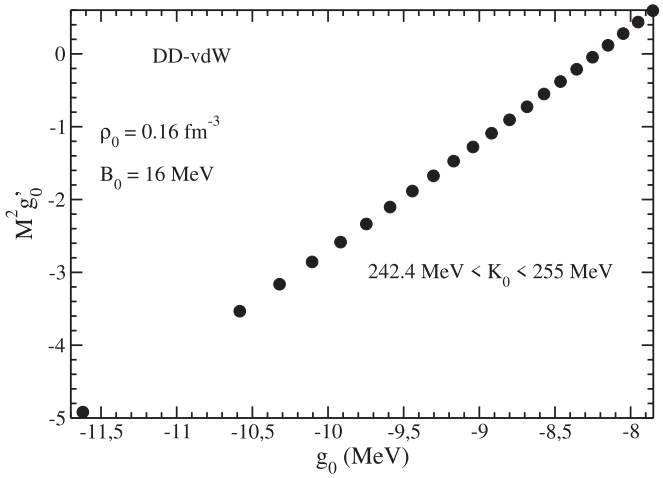

Figure 6. Correlation between $M^2 g_0'$ and g_0 for DD-vdW parametrizations consistent with the flow constraint.

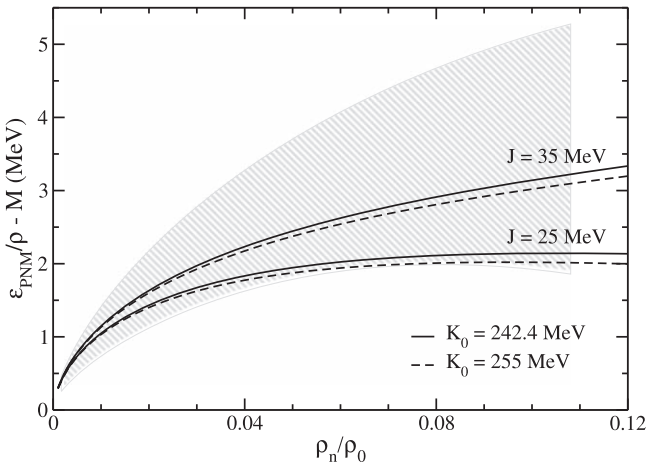

Figure 7. Density dependence of energy per particle in PNM for DD-vdW parametrizations consistent with the flow constraint. Band region: constraint given in [20, 47].

displayed in figure 7. One can see that the DD-vdW model is also consistent with this particular restriction.

Finally, we analyze the DD-vdW model against a constraint explored in [20, 47] related to the difference between proton and neutron densities (neutron skin thickness). In [48], the author associated this difference to the reduction of the symmetry energy at $\rho_0/2$ in terms of the quantity $r \equiv \mathcal{S}(\rho_0/2)/J$ and found the limit of $0.57 \leqslant r \leqslant 0.83$. This constraint is named as MIX4 in [20, 47]. In table 3, we show the values of $\mathcal{S}(\rho_0/2)/J$ for the parametrizations of the DD-vdW model consistent with the J and the flow constraints.

From table 3, one can verify that all parametrizations present numbers out of the limit of the MIX4 constraint. However, to follow the same criterion adopted in [20, 47] for that

Table 3. Values of r for DD-vdW parametrizations presenting 242.4 MeV $\leqslant K_0 \leqslant$ 255 MeV and 25 MeV $\leqslant J \leqslant$ 35 MeV.

K_0 (MeV)	J (MeV)	r
242.4	25	0.56
242.4	35	0.54
255	25	0.55
255	35	0.53

Table 4. Set of updated constraints (SET2a) used in [20] and applied to the DD-vdW model. See that reference for more details concerning each constraint.

Constraint	Quantity	Density region	Range of constraint
SM1	K_0	at ρ_0	190–270 MeV
SM3a	$P(\rho)$	$2 < \frac{\rho}{\rho_0} < 5$	Band region
SM4	$P(\rho)$	$1.2 < \frac{\rho}{\rho_0} < 2.2$	Band region
PNM1	$\mathcal{E}_{\rm PNM}/\rho$	$0.017 < \frac{\rho}{\rho_0} < 0.108$	Band region
MIX1a	J	at ρ_0	25–35 MeV
MIX2a	L_0	at ρ_0	25–115 MeV
MIX4	$\frac{\mathcal{S}(\rho_0/2)}{J}$	at ρ_0 and $\rho_0/2$	0.57–0.83

parametrizations do not satisfy only one of the analyzed constraints, we also establish here that a particular parametrization is approved if the value of the quantity exceeds the limits of the respective constraint by less than 5%. This is the case for the parametrizations reported in table 3, except for that presented in the last line. Therefore, one can conclude that the DD-vdW model also predicts parametrizations in agreement with this particular constraint.

5. Summary and conclusions

In this paper, we revisited the recently proposed density-dependent van der Waals model (DD-vdW) [17] by submitting it to the symmetric and asymmetric nuclear matter constraints used in [20]. The constraints used are summarized in table 4 as follows.

In order to become the model capable to reach the high-density regime, the new density dependent attractive interaction is considered, see equation (18). The new free parameter, n, is used to fix the value of the incompressibility at the saturation density. The other ones, found at the SNM regime, namely, a and b, are found by imposing the model to present the $B_0 = 16$ MeV at $\rho = \rho_0$. By imposing the model to satisfy the flow constraint [15], see figure 2, K_0 is found to be restricted to 242.4 MeV $\leqslant K_0 \leqslant$ 255 MeV, values compatible with the SM1 constraint. It also overlaps with the restriction proposed in [29], namely, 250 MeV $\leqslant K_0 \leqslant$ 315 MeV.

The last free parameter, d, is adjusted to generate parametrizations in which 25 MeV $\leqslant J \leqslant$ 35 MeV. Therefore, the model automatically satisfies the constraint named as MIX1a. All the other constraints are fully satisfied, excepting the MIX4. However, some parametrizations are out of its range only by less than 5%, which makes this constraint also satisfied, according to the criterion adopted in [20, 47].

We also analyzed the correlations between the bulk parameters in this model. It was shown that the crossing point in the $K(\rho)$ function, see figure 4(a), is related to the linear correlation between K_0 and the skewness coefficient at $\rho = \rho_0$, see figure 4(b). For the isovector sector, we also verified the linear correlation between J and L_0 (slope parameter at $\rho = \rho_0$), according to equation (28) and figure 5(a). Furthermore, a linear correlation between $3J - L_0$ and $K_{\rm sym}^0$ (symmetry energy curvature at $\rho = \rho_0$) also arises for the DD-vdW model, as shown in figure 5(b). This kind of correlation was also studied for relativistic and non-relativistic mean-field models in [44–46].

In [17], it was shown that this new proposed model, with only 4 free parameters, satisfactorily describes the constraints related to the binary neutron star merger event named as GW170817, and reported by the LIGO and Virgo collaboration [18, 19]. Here, we continued the analysis of the model and found that the mainly symmetric and asymmetric nuclear matter constraints are also satisfied, with some correlations between bulk parameters also observed.

Acknowledgments

This work is a part of the project INCT-FNA Proc. No. 464898/2014-5, partially supported by Conselho Nacional de Desenvolvimento Científico e Tecnológico (CNPq) under grants 310242/2017-7 and 406958/2018-1 (OL) and 433369/2018-3 (MD), and by Fundação de Amparo à Pesquisa do Estado de São Paulo (FAPESP) under thematic projects 2013/26258-4 (OL) and 2017/05660-0 (OL, MD).

ORCID iDs

M Dutra https://orcid.org/0000-0001-7501-0404
O Lourenço https://orcid.org/0000-0002-0935-8565

References

[1] Skyrme T H R 1956 *Phil. Mag.* **1** 1043
[2] Skyrme T H R 1959 *Nucl. Phys.* **9** 615
[3] Walecka J D 1974 *Ann. Phys.* **83** 491
[4] Serot B D and Walecka J D 1979 *Phys. Lett.* B **87** 172
[5] Serot B D and Walecka J D 1986 *Adv. Nucl. Phys.* **16** 1
[6] Stone J R, Miller J C, Koncewicz R, Stevenson P D and Strayer M R 2003 *Phys. Rev.* C **68** 034324
[7] Glendenning N K 2000 *Compact Stars* 2nd edn (New York: Springer)
[8] Lourenço O, Dutra M and Menezes D P 2017 *Phys. Rev.* C **95** 065212
[9] Lourenço O, Santos B M, Dutra M and Delfino A 2016 *Phys. Rev.* C **94** 045207
[10] Greiner W, Neise L and Stöker H 1995 *Thermodynamics and Statistical Mechanics* (New York: Springer)
[11] Landau L D and Lifshitz E M 1975 *Statistical Physics* (Oxford: Pergamon)
[12] Vovchenko V, Anchishkin D V and Gorenstein M I 2015 *J. Phys. A: Math. Theor.* **48** 305001
[13] Vovchenko V, Anchishkin D V and Gorenstein M I 2015 *Phys. Rev.* C **91** 064314
[14] Vovchenko V 2017 *Phys. Rev.* C **96** 015206
[15] Danielewicz P, Lacey R and Lynch W G 2002 *Science* **298** 1592
[16] Bugaev K A 2008 *Nucl. Phys.* A **807** 251
[17] Lourenço O, Dutra M, Lenzi C H, Bhuyan M, Biswal S K and Santos B M 2019 *Astrophys. J.* **882** 67
[18] Abbott B P *et al* (The LIGO Scientific Collaboration and the Virgo Collaboration) 2017 *Phys. Rev. Lett.* **119** 161101

[19] Abbott B P *et al* (The LIGO Scientific Collaboration and the Virgo Collaboration) 2018 *Phys. Rev. Lett.* **121** 161101
[20] Dutra M, Lourenço O, Avancini S S, Carlson B V, Delfino A, Menezes D P, Providência C, Typel S and Stone J R 2014 *Phys. Rev.* C **90** 055203
[21] Redlich O and Kwong J N S 1949 *Chem. Rev.* **44** 233
[22] Soave G 1972 *Chem. Eng. Sci.* **27** 1197
[23] Peng D-Y and Robinson D 1985 *Ind. Eng. Chem. Fundam.* **15** 59
[24] Vovchenko V, Gorenstein M I and Stoecker H 2018 *Eur. Phys. J.* A **54** 16
[25] Carnahan N F and Starling K E 1969 *J. Chem. Phys.* **51** 635
[26] Sagun V V *et al* 2018 *Eur. Phys. J.* A **54** 100
[27] Bugaev K A *et al* 2019 *Universe* **5** 63
[28] Steiner A W, Lattimer J M and Brown E F 2013 *Astrophys. J. Lett.* **765** L5
[29] Stone J R, Stone N J and Moszkowski S A 2014 *Phys. Rev.* C **89** 044316
[30] Garg U and Colò G 2018 *Prog. Part. Nucl. Phys.* **101** 55
[31] Lynch W G, Tsang M B, Zhang Y, Danielewicz P, Famiano M, Li Z and Steiner A W 2009 *Prog. Part. Nucl. Phys.* **62** 427
[32] Fuchs C 2006 *Prog. Part. Nucl. Phys.* **56** 1
[33] Cai B-J and Chen L-W 2017 *Nucl. Sci. Tech.* **28** 185
[34] Santos B M, Dutra M, Lourenço O and Delfino A 2015 *Phys. Rev.* C **92** 015210
[35] Khan E and Margueron J 2013 *Phys. Rev.* C **88** 034319
[36] Steiner A W, Lattimer J M and Brown E F 2010 *Astrophys. J.* **722** 33
[37] Farine M, Pearson J M and Tondeur F 1997 *Nucl. Phys.* A **615** 135
[38] Li B-A and Han X 2013 *Phys. Lett.* B **727** 276
[39] Baldo M and Burgio G F 2016 *Prog. Part. Nucl. Phys.* **91** 203
[40] Santos B M, Dutra M, Lourenço O and Delfino A 2014 *Phys. Rev.* C **90** 035203
[41] Holt J W and Lim Y 2018 *Phys. Lett.* B **784** 77
[42] Lalazissis G A *et al* 2009 *Phys. Lett.* B **671** 36
[43] Fattoyev F J, Newton W G, Xu J and Li B A 2012 *Phys. Rev.* C **86** 025804
[44] Mondal C, Agrawal B K, De J N, Samaddar S K, Centelles M and Viñas X 2017 *Phys. Rev.* C **96** 021302R
[45] Mondal C, Agrawal B K, De J N and Samaddar S K 2016 *Phys. Rev.* C **93** 044328
[46] Margueron J and Gulminelli F 2019 *Phys. Rev.* C **99** 025806
[47] Dutra M, Lourenço O, Sá Martins J S, Delfino A, Stone J R and Stevenson P D 2012 *Phys. Rev.* C **85** 035201
[48] Danielewicz P 2003 *Nucl. Phys.* A **727** 233